Physics – Uspekhi **67** (8) 803 – 813 (2024)

REVIEWS OF TOPICAL PROBLEMS

PACS numbers: **51.50. + v, 52.80. – s, 79.70. + q**

ON THE 90TH ANNIVERSARY OF THE P.N. LEBEDEV PHYSICAL INSTITUTE (LPI)

Conditions for the generation of runaway electrons in an air gap with an inhomogeneous electric field: theory and experiment

N M Zubarev, G A Mesyats, M I Yalandin

DOI: https://doi.org/10.3367/UFNe.2023.11.039608

Contents

Abstract. Conditions for the generation of runaway electrons (RAEs) in a magnetically insulated coaxial air diode with graphite cathodes of different geometries — needle and conical with a Taylor opening half angle of 49.3° — are compared. The axial magnetic field allows the RAE beam to be focused on a current probe collector, thereby increasing the sensitivity of the recording technique in use. The threshold RAE generation voltage for the Taylor cone is found to be lower than that for the needle (i.e., a cone with a small opening angle), which indicates its nonmonotonic angular dependence with a minimum at an angle not exceeding the Taylor angle. According to our estimates, the dynamics of free electrons change qualitatively at the Taylor angle. At large angles, they accelerate throughout the entire gap; at smaller angles, they accelerate near the cathode and then slow down at the periphery.

Keywords: runaway electrons, air diodes, inhomogeneous electric fields, guiding magnetic fields, pulsed breakdown, conical cathodes, Taylor angle

1. Introduction

The effect of runaway electrons [1–8] — their continuous acceleration in a gas or a plasma medium in a sufficiently strong external electric field — can be used to generate picosecond [9–13] beams of fast electrons with an energy of tens to hundreds of keV [14–22]. In a homogeneous electric field, electrons undergo a massive transition to the runaway regime if the field strength E exceeds a certain threshold value E_c, which depends on the type of gas and its density [3, 8, 23–25]. In atmospheric pressure air, according to [23, 26], $E_c \approx 270$ kV cm^{-1} (the authors of Refs [24, 27] report a value of 450 kV cm^{-1}; see also the results of numerical simulation [28–31]). The presence of the threshold is due to the fact that the braking (friction) force F acting on an electron in a medium is limited from above. It reaches a certain maximum F_{max} at an electron kinetic energy (ε) on the order of 100 eV. For air, the maximum occurs at an energy $\varepsilon_c \approx 110$ eV [24, 32] (the authors of Refs [23, 26] report a higher value of 150 eV). If the electric force eE acting on the electron (here, e is the elementary charge) exceeds F_{max}, then it will begin to continuously accelerate (i.e., to run away) regardless of its initial energy. In particular, low-energy thermal electrons may run away, as a result of which this regime is often called 'cold runaway' [25]. Accordingly, the condition for the runaway of initially thermal electrons is $E > E_c = F_{max}/e$.

In laboratory experiments with runaway electrons (RAEs), use is often made of inhomogeneous field distributions [12, 14, 33–38]. The use of pointed (needle, blade, conical, tubular edge, etc.) cathodes provides a significant local field enhancement in the cathode region and facilitates the transition of free electrons to the runaway regime: in an inhomogeneous field, it occurs at significantly lower voltages than in a homogeneous one. Recent theoretical studies [39–43] have indicated that, for field distributions with varying degrees of inhomogeneity, the transition of electrons to the runaway regime can be determined by various criteria; the condition that the field strength near the cathode exceeds the value E_c turns out to be only a necessary, but not sufficient, condition for the generation of RAEs in a field that rapidly decreases with distance from the cathode. Understanding the conditions for RAE generation is fundamentally important

N M Zubarev [1, 2, a], **G A Mesyats** [1, b], **M I Yalandin** [1, 2, c]
[1] Lebedev Physical Institute, Russian Academy of Sciences, Leninskii prosp. 53, 119991 Moscow, Russian Federation
[2] Institute of Electrophysics, Ural Branch of the Russian Academy of Sciences, ul. Amundsena 106, 620016 Ekaterinburg, Russian Federation
E-mail: [a] nick@iep.uran.ru, [b] mesyats@sci.lebedev.ru, [c] yalandin@iep.uran.ru

Received 9 October 2023, revised 15 November 2023
Uspekhi Fizicheskikh Nauk **194** (8) 853 – 864 (2024)
Translated by I A Ulitkin

for developing sources of fast electrons. For example, to generate a disk bunch of electrons, emissions of RAE flows from multiple concentric edge cathodes should be synchronized with picosecond accuracy [20]. This necessitates a detailed experimental and theoretical study of the conditions and features of RAE generation when using electrode systems of various configurations. This review is devoted to this topic.

Zubarev et al. [36] intentionally studied conditions for the generation of runaway electrons in a gas diode with an inhomogeneous field distribution due to the use of a tubular edge cathode. They used stainless steel cathodes with different edge thicknesses and found that, for a highly sharpened edge, the runaway threshold is determined not by the field value near the cathode but by the nonlocal condition that the potential difference applied to the gap exceed a certain value, depending on the interelectrode distance and gas parameters (it should be noted that the condition from [36] is not related to the nonlocal condition for the absence of Townsend electron multiplication, which the authors of Refs [44–46] proposed to use as a runaway criterion). Nevertheless, the experimental technique used in [36] had a number of disadvantages and can be improved.

First, it seems advisable to use graphite cathodes, which, due to the significant heterogeneity of the surface, have a much higher emissivity than that of steel cathodes. The relatively low emissivity of the steel surface, which changes noticeably in a long series of experiments due to smoothing of surface irregularities (i.e., surface conditioning), can be a factor influencing the conditions for the generation of runaway electrons [47, 48] due to the delay in the moment of emission of primary (field emission) free electrons. The use of a graphite cathode eliminates this factor and allows concentrating on processes in the gas and the generated plasma.

Second, systems have been recently developed that control RAE flows through a strong magnetic field of 1–5 T [14, 20, 49, 50]. Without a magnetic field, runaway electrons propagate mainly along the electric field lines. The significant divergence of the field lines when using pointed cathodes leads to the fact that the RAE flow expands to a significant solid angle on the order of π. As a consequence, the RAE flow density radically decreases with distance from the cathode. However, the size of the collector of the current sensor that records RAEs is limited to a millimeter scale, which is due to the need for picosecond time resolution [51]. In such a situation, only a small fraction of the total RAE flow reaches the sensor, which reduces the sensitivity of the RAE recording technique and, as a consequence, the accuracy of determining the threshold for RAE generation. When use is made of conical and needle-shaped cathodes and a guiding axial magnetic field that restrains the expansion of the RAE flow is applied, it becomes possible to deliver the entire RAE beam to a millimeter-sized collector [14], which eliminates the described problem.

The plan of this paper is as follows. Section 2 provides a preliminary analysis of the dynamics of free electrons in a gas in an electric field of varying degrees of inhomogeneity, the variation of which is ensured by changing the opening angle of the conical cathode. Based on the analysis, we identify the most interesting electrode configurations for experimental study of the conditions for generating runaway electrons. These studies require changing the near-cathode field strength over a wide range, which can be achieved by applying high-voltage subnanosecond pulses of controlled amplitude. Section 3 describes a technique for generating such pulses and a method for determining their characteristics at the cathode using a remote sensor; it also presents a magnetically insulated coaxial diode with atmospheric pressure air and replaceable (conical or needle) graphite cathodes. Section 4 reports the experimental results; the runaway conditions for gas gaps of various lengths are compared using cathodes of three configurations: needles with a rounded or pointed tip (cases of a highly inhomogeneous field) and a cone with an opening half angle of 49.3° (the case with a relatively weakly inhomogeneous field). Section 5 presents calculations of electron dynamics in gaps of real configurations. The calculated threshold field strengths are compared with experimental data. Section 6 contains our conclusions regarding the features of runaway electron generation at different degrees of field inhomogeneity, based on a comparison of theory and experiments.

2. Preliminary analysis and experimental tasks

To understand the problems posed in experiments and choose the commonly used cathode configurations, it is necessary to make several preliminary estimates.

Let us consider a cathode in the form of an ideal (with a zero radius of curvature of the tip) cone with an opening half angle α. Since RAEs are generated at the initial stage of breakdown development and their number under threshold runaway conditions is minimal, we can assume that they cross the gap when the electric field distribution is not yet distorted by the electric space charge (this distortion may be a reason for the appearance of 'anomalous' RAEs, whose energy exceeds the energy corresponding to the voltage applied to the gap [7, 52]). In the absence of a space charge, the electric field potential φ satisfies the Laplace equation with the condition of equipotentiality of the cathode surface. Without loss of generality, the cathode potential can be taken equal to zero; then, the anode potential will be positive. In spherical coordinates, the axially symmetric distribution of the field potential is given by the expression

$$\varphi = U\left(\frac{r}{D}\right)^{\gamma} P_{\gamma}(\cos\theta)\,. \tag{1}$$

Here, U is the potential difference applied to the gap, r is the distance from the cone apex, θ is the polar angle measured from the symmetry axis (the z-axis of the Cartesian coordinate system), D is the interelectrode distance, γ is an exponent characterizing the degree of field inhomogeneity, and P_{γ} is the Legendre function on the order of γ. The exponent γ is related to the angle α by the equation

$$P_{\gamma}(-\cos\alpha) = 0\,, \tag{2}$$

which arises from (1) as a consequence of the requirement that the cone surface be equipotential, $\varphi|_{\theta=\pi-\alpha} = 0$. According to (2), as α increases from zero (infinitely thin needle) to $\pi/2$ (plane), the exponent γ monotonically increases, running through values from zero to unity, $0 \leqslant \gamma \leqslant 1$. Thus, by choosing the opening angle of the cone, we regulate the degree of inhomogeneity of the field distribution over a wide range.

Obviously, the z direction (i.e., $\theta = 0$) is the most favorable for the electron runaway. Therefore, we limit ourselves to considering the propagation of electrons along

the z-axis. As follows from (1), the electric field potential satisfies the power law $\varphi \propto z^{\gamma}$ and, therefore, the absolute value of the field strength E decreases with distance z from the cathode edge as $E \propto z^{\gamma-1}$. At $z \to 0$, the field strength formally tends to infinity (the exception is the trivial case of a homogeneous field, $\gamma = 1$), i.e., obviously exceeds the runaway threshold E_c. An electron starting from the edge then begins to run away in the near-cathode region. However, the question is whether it will continue to accelerate in the region of high z where the field strength becomes low or it will lose energy and become thermal.

We will start with the assumption that the inequality $eE \gg F$ is valid on the periphery; i.e., the electrical force dominates the frictional force and, as a consequence, the electron is continuously accelerated. In this case, the kinetic energy of the electron can be estimated by the potential difference it has passed through: $\varepsilon \approx e\varphi \propto z^{\gamma}$. For the friction force, according to the Bethe formula [53], we obtain at the periphery in the basic order (without taking into account weak logarithmic corrections) $F \propto \varepsilon^{-1} \propto z^{-\gamma}$. Let us compare it with the electric force $eE \propto z^{\gamma-1}$. It is immediately clear that at $z \to \infty$ the condition $eE \gg F$ is valid only if $\gamma > 1/2$; i.e., the value of γ is in the range $1/2 < \gamma \leqslant 1$. For $0 \leqslant \gamma < 1/2$, the initial assumption about the dominance of the accelerating force eE over the braking force F for large z is violated. At such values of γ, the electron will not continuously accelerate. Its behavior turns out to be more complex: first, in the region of small z, it will accelerate, and then, moving away from the cathode to a sufficiently large distance, it will begin to decelerate. In the absence of restrictions on z, it will inevitably become thermal, with an energy less than ε_c.

Thus, our a priori analysis of the dynamics of free electrons in a gas under conditions of an inhomogeneous field showed that it should be radically different for $0 \leqslant \gamma < 1/2$ and for $1/2 < \gamma \leqslant 1$, i.e., as it is convenient to assume, in the cases of strongly and weakly inhomogeneous fields (see also [54]). The boundary case with $\gamma = 1/2$, i.e., when a decrease in the field with distance from the cathode tip follows the inverse square-root law $E \propto 1/\sqrt{r}$, corresponds, according to (2), to a cone with an opening half angle of 49.3°. This angle is called in the literature the Taylor angle; it arises when considering static [55, 56] and dynamic [57, 58] Taylor cone formations on the surface of a conducting liquid in an external electric field. The characteristic scaling of $E \propto 1/\sqrt{r}$ in these problems is ensured by the balance of electrostatic and capillary forces on the surface of the liquid cone. We will sometimes, for brevity, refer to a cone-shaped cathode with $\alpha = 49.3°$ as a Taylor cone, without implying any specificity associated with the use of conductive liquid electrodes.

Let us now discuss the difference between the cases $0 \leqslant \gamma < 1/2$ and $1/2 < \gamma \leqslant 1$ [conical cathodes with relatively small ($\alpha < 49.3°$) and, accordingly, large ($\alpha > 49.3°$) opening half angles] from the point view of the occurrence of ionization processes in the gas gap. The behavior of a free electron in the case of a weakly inhomogeneous field is generally similar to its behavior in a homogeneous field. If a thermal electron switches to the runaway regime, it will continuously accelerate throughout the entire interelectrode gap. Since the cross section for impact ionization of gas molecules decreases with increasing kinetic energy of the electron in the region $\varepsilon > \varepsilon_c$ approximately as $1/\varepsilon$ [24], the electron mainly ionizes the gas in the narrow near-cathode region. In the main part of the gap, where the electron gains an energy of tens of keV, i.e., orders of magnitude greater than ~ 110 eV, corresponding to the maximum ionization cross section (for nitrogen, it is approximately at the same energy as the maximum friction force [32]), ionization processes with the participation of RAEs proceed much more slowly and will not affect the conditions of their generation.

A completely different situation arises in a highly inhomogeneous field. Electrons undergo a transition to the runaway regime in a supercritical field in the cathode region. However, when they enter a weak field on the periphery, they, as already mentioned, begin to slow down. If their movement were not limited by the anode, they would turn into thermal ones at a certain distance L from the cathode, which depends on the voltage applied to the gap approximately as $L \propto U^2/\rho$ (this dependence follows from the Schonland formula [59] for the depth of penetration of the electron flow, accelerated by voltage U, into a substance — in our case, into a gas — with density ρ). Since the voltage across the gap in our experiments does not increase instantly but with a variable slope of the front, reaching a maximum of $(4-7) \times 10^{14}$ V s^{-1}, the distance L will increase with time. At the beginning of the pulse there will be $L < D$; i.e., the electrons will become thermal inside the gap. For brevity, we will call this regime of electron motion 'incomplete' runaway (a similar regime of motion of free electrons in an inhomogeneous field near an avalanche head was considered in [60]). As U increases to sufficiently high values, the inequality $L > D$ will be satisfied, i.e., the electrons, despite the deceleration, will reach the anode and will be recorded in the experiment as runaway electrons.

It is important that in the 'incomplete' runaway regime the rate of ionization processes in the main part of the gap increase dramatically: when the energy of decelerating electrons decreases to values comparable to ε_c, the ionization cross section of gas molecules sharply increases. The appearance of a significant number of secondary electrons and their subsequent avalanche multiplication at the leading edge of a voltage pulse lasting hundreds of picoseconds will lead to the formation of a fairly large region of an electric space charge, which will inevitably affect the conditions for subsequent RAE generation.

Thus, when use is made of conical cathodes with sufficiently large angles $49.3° < \alpha < 90°$, ionization processes in the main part of the gas gap are expected not to noticeably affect the conditions for the generation of runaway electrons. On the contrary, for sharper cathodes with $0° \leqslant \alpha < 49.3°$, one can expect that a sufficiently dense plasma will form in the near-cathode part of the gap, which will screen the field near the cathode and, as a consequence, lead to a delay in RAE generation (let us pay attention to the fundamental difference between the role of field screening here and that described in [12, 61–63], where screening caused the interruption of the RAE flow). As a result, runaway electrons will be generated at higher voltages than would occur in a Laplace field (meaning one that does not take into account the influence of the electric space charge).

The performed analysis determines our choice of cathode configurations used in the experiments. Some experiments will be carried out with a conical cathode with an opening half angle of 49.3° (Taylor cone). This angle corresponds to the most interesting case of $\gamma = 1/2$, which is the boundary one for weakly and strongly inhomogeneous field distributions in the gap. Starting from this angle, we can assume that the space

charge will not significantly affect the conditions for RAE generation. Therefore, it is possible to conduct, in a certain sense, a 'pure' experiment, excluding the space charge factor. From general considerations, it is clear that increasing the degree of field inhomogeneity simplifies the transition of electrons to the runaway regime and leads to a decrease in the threshold voltage. As a consequence, from the region of angles from 49.3° to 90°, corresponding to a weakly inhomogeneous field, it is advisable to use the sharpest, Taylor angle. The experimental data obtained for such a cathode can be considered as reference data.

Another cathode configuration, the advisability of which follows from our analysis, is a needle cathode, in fact, a cone with a minimum possible opening angle. When using a needle cathode, the influence of a space charge on the conditions for electron runaway will be the most pronounced. Comparing this case with the 'reference' case — with the case of the Taylor cone — will make it possible to isolate the factor of the influence of the space charge on the conditions for RAE generation. For a Laplace field, sharpening the cathode would lead to a decrease in the electron runaway threshold. The influence of the space charge causes the opposite trend — an increase in the threshold voltage with sharpening of the cathode. It is clear that it is impossible to practically implement the situation with $\gamma \to 0$. The case implemented in experiments (for details, see Sections 3 and 5) allows a power-law approximation for the field distribution with $\gamma \approx 0.21$, which, according to (2), can be interpreted as a fairly thin cone with an opening half angle of $\alpha \approx 11°$.

Previously, Zubarev et al. [43] showed theoretically that, at a threshold value $R_c \approx 500$ μm of radius R of the needle cathode tip, a radical change occurs in the nature of the dependence of the threshold voltage U_c of runaway electron emission on R ($D = 10$ mm was taken; the gas was air at atmospheric pressure). The change is due to a change in the runaway criterion. The local condition of the field exceeding the critical value E_c at the cathode determines the RAE generation threshold only for quite blunt needles with $R > R_c$ (slightly inhomogeneous field distribution). At $R < R_c$ (highly inhomogeneous field distribution), the runaway condition has a nonlocal character — what is important are the dynamics of electrons throughout the gap, including at the periphery, in the weak field region. At threshold voltages (U_c) for observing runaway electrons at the anode, the electric field near the tip with $R < R_c$ can significantly exceed the critical one (E_c), typical of initial thermal electrons in a gap with a homogeneous field. The described result corresponds to the Laplace field. The influence of the electric space charge, as follows from our estimates, should lead to an increase in the threshold voltage U_c and, as a consequence, to an even greater excess of the value of E_c by the field strength at the tip. Studying this effect is also the goal of our experiments.

3. Technique and methodology of experiments

In experiments on determining the RAE emission threshold U_c in a gas diode with gaps D equal to 10 and 30 mm, amplitude-controlled high-voltage pulses with an FWHM duration ($\tau_{1/2}$) of at least $2D/c$ are needed. Factor '2' approximately takes into account the reduced velocity of RAEs in comparison with the speed of light c. For a larger gap, $D = 30$ mm, this yields $\tau_{1/2} \geqslant 200$ ps. Such pulses are generated using the setup shown in Fig. 1a.

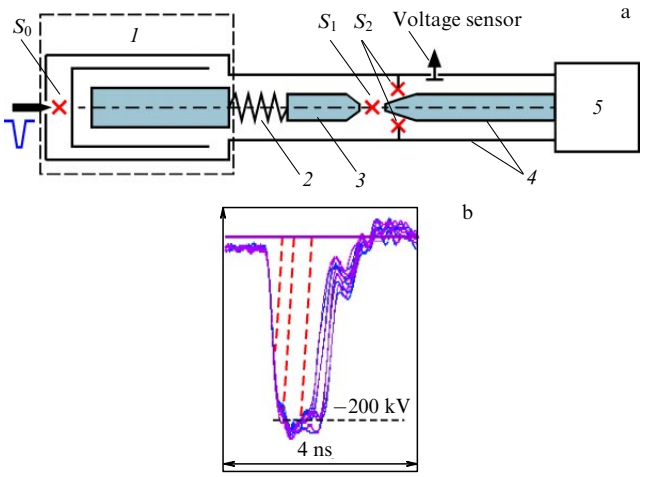

Figure 1. (a) Schematic of setup and (b) generated pulses with smooth tuning of amplitude and duration (slanted dashed lines) with variation in breakdown voltage of chopping spark gap. Designations: *1* — nanosecond high-voltage driver; *2* — charging inductance; *3* — forming line; *4* — coaxial transmission line with oil insulation; *5* — load: coaxial gas diode with magnetic insulation; S_0 — controlled nitrogen (40 atm) spark gap of the driver; and S_1, S_2 — sharpening and chopping nitrogen (60 atm) spark gaps of pulse converter, respectively.

A pulse from the RADAN-303 driver with a double forming line (DFL) [64], after switching the controlled spark gap S_0, charges the short forming line (FL) of the converter [65] in ~ 5 ns. The DFL is pre-charged in a time of ~ 8 μs using a Tesla transformer. After the uncontrolled sharpening spark gap S_1 is triggered, a pulse (Fig. 1b) with an FWHM duration of ~ 1 ns and a subnanosecond front is supplied from the FL to the transmission line (TL) with a wave impedance of ~ 43 Ω. The amplitude of this pulse (−200 kV, Fig. 1b) can be reduced to tens of kilovolts by adjusting the triggering moment of the driver spark gap to < 8 μs, as well as by reducing the gap S_1. Below, we will talk about the amplitudes of negative voltage pulses 'in absolute values.' At a high overvoltage rate of the gap in the chopping spark gap S_2, if it is triggered at an appropriate gap setting, the trailing edge (cut) of the shortened pulse turns out to be shorter than the leading edge. In the experiments described below, we set the amplitude of the voltage pulse on the load — a gas diode (GD) — precisely by varying the gap S_2. As shown by the slanted dashed lines in Fig. 1b, as the amplitude of the pulse decreases, its duration also decreases. The choice of adjustment by setting the breakdown voltage S_2 is explained by the fact that the spark gap S_1 has an interelectrode capacitance, and therefore, before the main pulse, a voltage prepulse with an amplitude of about 10 kV arrives at the TL. Considering the objectives of our experiments, the prepulse parameters cannot be changed; i.e., the gap S_1 must be fixed. Indeed, it is known in [15] that the conditions for initiation of near-cathode plasma by field emission electrons from the cathode and, consequently, the total RAE current will significantly depend on the amplitude and duration of the prepulse. Figure 2 shows typical oscillograms demonstrating the possibilities of adjusting the amplitude and duration of voltage pulses using a chopping spark gap.

An important problem in assessing the RAE emission threshold is determining the value of U_c for voltage pulses at the GD cathode. It is impossible to place any contactless

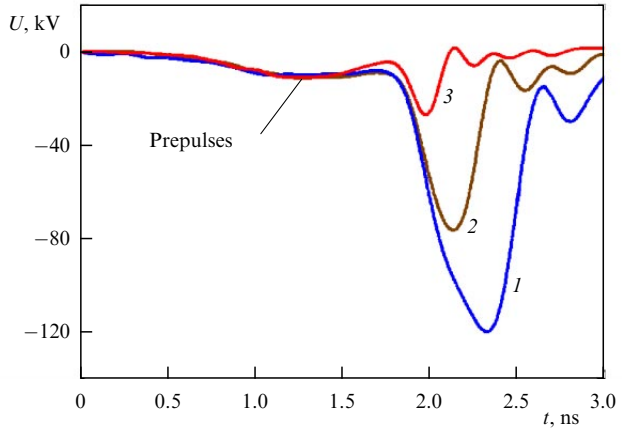

Figure 2. Variation by adjusting chopping spark gap of voltage pulse supplied to load via transmission line. Sequence of pulses *1*, *2*, and *3* corresponds to a decrease in gap of spark gap S_2 (Fig. 1).

sensor at the cathode due to the problems of random breakdowns. Therefore, to obtain information about U_c, we analyze the voltage pulses reflected from the GD. The coaxial path, which continues the TL inside the GD, changes the wave impedance in front of the cathode, i.e., it is heterogeneous. Because of this, the dynamic time domain reflectometry [66] cannot be applied to accurately determine U_c. In addition, such measurements are complicated by the presence of noise accompanying the trailing edge of the incident pulse. Under such conditions, we numerically simulated (KARAT code) pulse delivery (curve *3* in Fig. 2) from the TL to the cathode with subsequent reflection. The obtained data (Fig. 3a) show that the front of the reflected pulse is distorted insignificantly, and its amplitude is reduced by approximately 7% relative to the amplitude of the incident pulse. In experiments with an incident pulse FWHM duration of ~ 200 ps, we observed the return of reflections with a decrease in amplitude with a typical factor of 0.8 (Fig. 3b). The reason for the greater (greater than in the calculation) reduction in reflection amplitude is the loss in the dielectric of a sufficiently long TL between the sensor and the cathode. Thus, there is reason to believe that pulses with an amplitude with a factor of $\sqrt{0.8} \approx 0.9$ relative to the pulse amplitude measured by the voltage sensor in the recording region are incident on the cathode. The sensor was specially located in the TL region, remote from the GD, in order to delay the reflection relative to the noise following the trailing edge of the incident pulse.

An important feature in recording threshold voltage regimes of RAE emission is that, with a sufficiently short duration of the incident pulse, the reflected pulse practically repeats its shape (Fig. 3b). In particular, the reflection does not have a polarity reversal, which usually manifests itself already at the beginning of the development of breakdown initiated by the passage of high-current RAEs to the anode. This means that the measured RAE threshold currents were small and the resulting ionization wave did not create sufficient conductivity to ensure significant distortion of the electric field distribution in the GD, specified by the incident voltage pulse, providing a basis for calculating electric fields in the absence of effects associated with the possible presence of a space charge of the electron flow in the main part of the

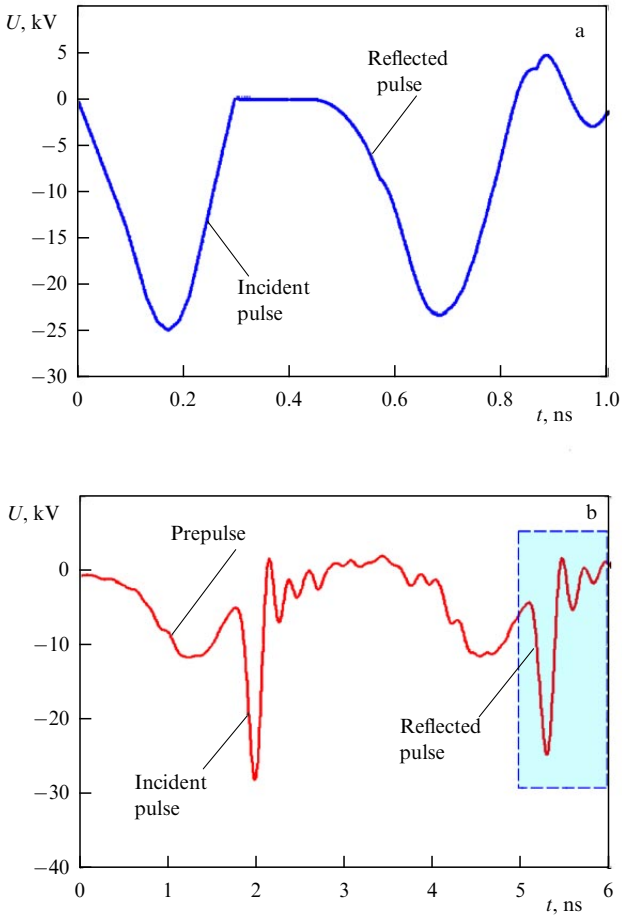

Figure 3. (a) Numerical model of reflection — in idle regime — of a short incident voltage pulse from cathode system in the form of a Taylor cone. Prepulse is not shown. (b) Typical reflection in experiment in RAE emission regime.

gap of the GD (as happens in vacuum diodes [67]) and a dense ionization trace after the passage of relatively large-current RAEs.

Figure 4 shows the air-filled diode configurations used in the experiments. The gaps D were 10 or 30 mm. The coaxial supply TL in the gas section had a diameter ratio of 45/22, which corresponded to a characteristic impedance of 43 Ω. The same wave impedance was in the region of a specially profiled bushing and in the region of the oil-insulated TL, where the capacitive voltage sensor was installed. Thus, there were no spurious signals when the voltage pulse reflected from the GD was recorded.

Cathodes in the form of a cone or needle were made of graphite. This material was chosen because it is formed from compressed microparticles. Unlike the vacuum regime of high-current explosive electron emission [68], the microscopic structure of the cathode surface in the GD is restored each time it is switched on due to the entrainment of graphite. Note that on metal cathodes there is also melting of microprotrusions, the number of which is initially much smaller than for graphite, and they provide a significantly lower field amplification factor on the emission surface. As a consequence, all other things being equal, when using graphite, RAE generation begins somewhat earlier than in the case of metal cathodes, and it is more stable in time — the spread of RAE current fronts is usually a few picoseconds [50].

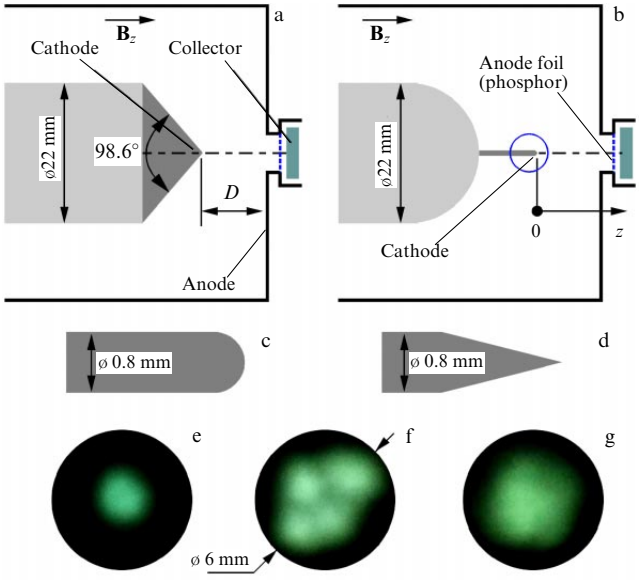

Figure 4. Geometry of GD with (a) conical (opening half angle of 49.3°) and (b) needle-shaped graphite cathodes. (c, d) Variants of tip profiles of needle cathodes. Induction of longitudinal magnetic field $B_z = 2$ T in all cases. (e–g) Glow of Gd_2O_2S:Tb phosphor installed in anode plane ($D = 30$ mm) under the influence of magnetized RAE flows formed near cathode tips (a, c, d), respectively.

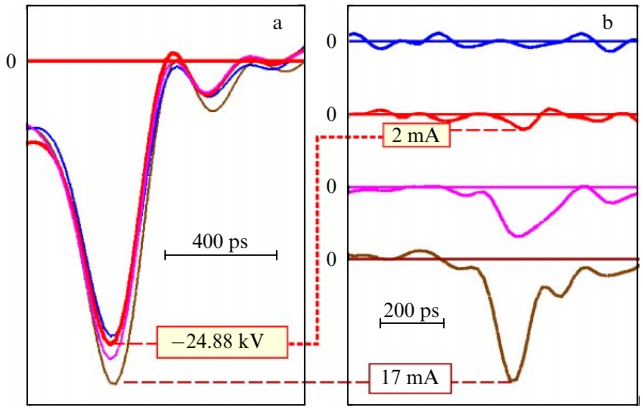

Figure 5. (a) Variation in amplitudes of reflected voltage pulses, in the range of which threshold for appearance of RAE current in GD was measured at a gap of $D = 30$ mm. (b) RAE currents recorded by collector sensor. Beam second from top (red) is threshold current against background of oscilloscope noise. Oscilloscope bandwidth is 6 GHz.

The RAE current at the anode was measured using a collector sensor with a design similar to that described in [12, 51, 69]. In order for all accelerated runaway electrons to be focused on the sensor collector having a diameter of 9 mm, we, as in [14], applied a longitudinal magnetic field with an induction of ~ 2 T, generated by a pulsed solenoid. The focusing of the RAEs is demonstrated in Figs 4e–4g. Shown here is the glow of the phosphor located at the anode, observed under the influence of magnetized RAE flows for different cathode profiles (Figs 4a, 4c, and 4d, respectively). The amplitudes of the incident voltage pulses (in the range between pulses *1* and *2* in Fig. 2) and their reflections from the cathodes noticeably exceeded values sufficient for the appearance of runaway electrons. An increased voltage amplitude was required because the response of the Gd_2O_2S:Tb phosphor to the action of fast electrons depends on many factors (energy, current density, and duration) [70] and in our case (for measuring U_c) was not calibrated. Let us note that the narrowest RAE flow is typical of a conical cathode (Fig. 4a), while needle-shaped cathodes (Figs 4c and 4d) provide a broadened flow. The reason for this broadening may be the larger scales of the space charge region near the cathode due to the implementation of the regime of 'incomplete' electron runaway. Also noteworthy is the presence of an internal structure of the RAE flow in the case of a rounded needle (Fig. 4f). This is apparently explained by the presence of several emission zones due to the larger working surface of the cathode and the smaller difference in the electric field at the axis and at the periphery than in the case of a sharp needle (Fig. 4g).

Using the current signals from the collector sensor, we established that there were no conditions for RAE emission by a nanosecond voltage prepulse with an amplitude of ≈ 10 kV (Fig. 3b). Runaway electrons manifesting themselves in the form of a current surge always occurred at high voltages and were 'tied' to the region of a short peak following the prepulse.

4. Experimental results and discussion

At the first stage of the experiments, the RAE emission voltage (U_c) was determined in a diode with a graphite cathode in the form of a Taylor cone for distances of 10 and 30 mm to the anode constriction. As an example, such measurements are presented in Fig. 5 for a gap of 30 mm. A current signal of ≈ 2 mA from the sensor (with an RAE charge of ≈ 0.2 pC) was observed against the background of oscilloscope noise (second beam from the top in Fig. 5b), when the voltage amplitude of the reflected pulse (Fig. 5a) was 24.88 kV. Deviations in the voltage amplitude of a few percent led to a significant increase in the current or, conversely, to its disappearance (the two lower and upper beams in Fig. 5b, respectively). Voltage pulses in Fig. 5a are shown in the region highlighted in Fig. 3b by a dashed (halftone) rectangle. Taking into account the attenuation factor in the path (0.9) and doubling the voltage in the idle regime before RAE emission or in its absence, a voltage of 55.8 kV was reached at the cathode. Similar measurements of voltages U_c at which RAEs were observed were performed for all configurations of the cathodes presented in Fig. 4 at gaps of 10 and 30 mm. The obtained data are summarized in Table 1. It also shows the values of the field strength at a control point located 50 μm from the cathode, calculated in the electrostatic approximation [71] without taking into account the influence of the space charge for threshold voltages (we denote this field as E_0). This choice of the control point is due to the fact that the main RAE flow is formed not at the cathode but at the outer boundary of a narrow plasma region that appears in the vicinity of the cathode [61, 62]. According to the results of numerical simulations for various cathode configurations [12, 63], a sufficiently dense plasma, ensuring potential equalization (field displacement), is formed in the region $25 < z < 75$ μm at the tip apex. This allows us to take the point $z = 50$ μm as a basis for estimates.

Let us consider the field distributions calculated for the recorded threshold peak voltages (Fig. 6). It follows from the data in Table 1 and distributions $E(z)$ in Fig. 6a that only for a cathode in the form of a Taylor cone does the field strength at a distance $z = 50$ μm from the cathode edge (E_0) fall within the range of critical values proposed in the literature — from 270 kV cm^{-1} according to [23, 26] to 450 kV cm^{-1} according

Table 1. Experimental values of the RAE emission voltage (U_c) and fields (E_0) at a point spaced away from the cathode by 50 μm.

	10-mm gap	30-mm gap
Taylor cone	$U_c = 44.6$ kV; $E_0 = 340$ kV cm^{-1}	$U_c = 55.8$ kV; $E_0 = 375$ kV cm^{-1}
Rounded needle	$U_c = 63.2$ kV; $E_0 = 720$ kV cm^{-1}	$U_c = 68.5$ kV; $E_0 = 725$ kV cm^{-1}
Sharp needle	$U_c = 62.8$ kV; $E_0 = 1050$ kV cm^{-1}	$U_c = 69.9$ kV; $E_0 = 1090$ kV cm^{-1}

to [24, 27]. We have $E_0 = 340$ and 375 kV cm^{-1} for $D = 10$ and 30 mm, respectively (see also curves E_5 and E_6 in Fig. 6). For both a rounded needle and a pointed needle, the field strength E_0 is several times higher than E_c. This indicates the inapplicability of the local condition $E_0 > E_c$ as a criterion for the generation of runaway electrons under conditions of a highly inhomogeneous electric field (see also Sections 2 and 5 with theoretical analysis, and studies [39–43]).

Note that the runaway threshold voltages for rounded and pointed needles at the same gaps turn out to be almost identical: 63.2 and 62.8 kV for $D = 10$ mm and 68.5 and 69.9 kV for $D = 30$ mm (Table 1). At the same time, the field strengths at the control point $z = 50$ μm are noticeably different: 720 and 1050 kV cm^{-1} for $D = 10$ mm and 725 and 1090 kV cm^{-1} for $D = 30$ mm (Table 1 and Fig. 6a). This indicates that the details of the electric field distribution in the immediate vicinity of the tip of the needles do not have a decisive impact on the conditions for RAE generation. The runaway threshold is primarily determined by the potential difference applied to the gap. Thus, the condition for electron runaway turns out to be nonlocal.

It is clear from Fig. 6 that the $E(z)$ dependences corresponding to the runaway threshold for each of the three studied cathode configurations coincide with good accuracy for both gaps of 10 and 30 mm (i.e., the field distributions in pairs E_1 and E_2; E_3 and E_4; and E_5 and E_6 coincide). Obviously, due to the different lengths of the gaps, only the regions $0 < z < 10$ mm can be compared (Fig. 6b). This coincidence is natural and is the result of scaling the problem parameters. The dynamics of electron runaway, and in particular the runaway threshold, are determined by the electric field distributions. It should be expected that, if the field distributions generally coincide, as is the case for the three pairs in Fig. 6, then the processes associated with electron runaway will proceed identically. If one of the field distributions turns out to be the threshold for RAE generation, then the other distribution will also correspond to the runaway threshold. An increase in the interelectrode distance for a given cathode configuration will then require (to maintain threshold conditions for the generation of runaway electrons) an increase in the applied potential difference. In any case, the pairwise coincidence of the field distributions indicates that the experimental technique used to determine the runaway threshold voltages (U_c) provides stable and predictable results.

An interesting result, which was indicated by our preliminary analysis in Section 2, is that the threshold runaway voltages for a Taylor cone turned out to be noticeably lower than those for needles of both configurations: more than ~ 1.4 and ~ 1.2 times for $D = 10$ and 30 mm, respectively (see Table 1). In a Laplace electric field, it would be natural to expect the opposite tendency, i.e., a decrease in the runaway

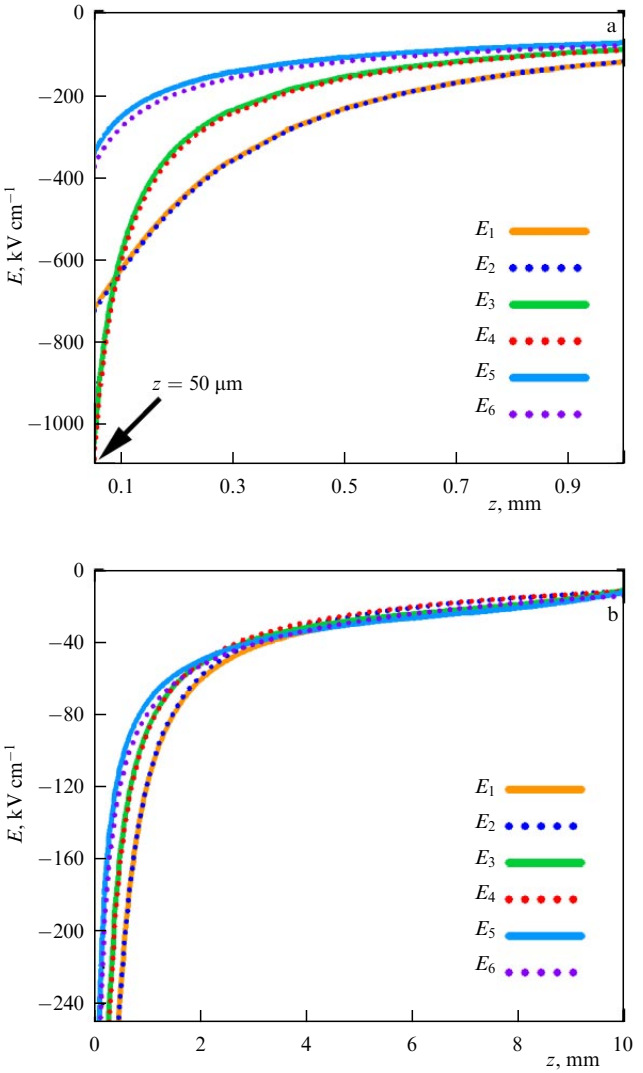

Figure 6. Field distributions in electrostatic approximation at peak 'threshold' voltages given in Table 1: E_1 — rounded needle, $D = 10$ mm; E_2 — rounded needle, $D = 30$ mm; E_3 — sharp needle, $D = 10$ mm; E_4 — sharp needle, $D = 30$ mm; E_5 — Taylor cone, $D = 10$ mm; and E_6 — Taylor cone, $D = 30$ mm.

voltage with an increase in the degree of field inhomogeneity, in particular, when moving from a Taylor cone to a thin needle as a cathode [54]. Features of electron dynamics in a sharply inhomogeneous field in the vicinity of the needle (the 'incomplete' runaway regime) can cause the formation of a space charge in the initial part of the gap, with the charge screening the submillimeter region of the enhanced field at the cathode (Fig. 6a) and, as a consequence, complicating the runaway of electrons.

The fact that the threshold runaway voltage for the Taylor cone is lower than that for the needle indicates its nonmonotonic dependence on the opening angle of the conical cathode. It follows from general considerations that the maximum voltage will be for the trivial case of a homogeneous field corresponding to a cone with $\alpha = 90°$ (it is estimated as $E_c D$; for $E_c = 270$ kV cm^{-1}, we have $U_c = 270$ and 810 kV at $D = 10$ and 30 mm, respectively). As the cone becomes sharper, the voltage decreases in the region of large angles and then increases in the region of small angles, when the cone turns into a needle. Based on our analysis from Section 2,

which indicates a change in the nature of the RAE dynamics at a Taylor angle, we can assume that the minimum will occur at $\alpha \leqslant 49.3^\circ$.

5. Simulation of electron runaway dynamics

Let us consider the dynamics of free electrons in GD gaps. The one-dimensional (along the z-axis) motion of an electron with kinetic energy ε in a gas under the action of an electric field E is described by the equation [8, 23]

$$\frac{\partial \varepsilon}{\partial z} = -eE(z,t) - F(\varepsilon)\,. \tag{3}$$

For the dependence of the friction force of an electron in a gas on its energy, we will use the approximation

$$F(\varepsilon) = \begin{cases} eE_c \sqrt{\dfrac{4e\varepsilon}{9\varepsilon_c}}\,, & \varepsilon < \varepsilon_0 \equiv e^{-1/3}\,\varepsilon_c\,, \\ eE_c \dfrac{\varepsilon_c}{\varepsilon} \ln\left(\dfrac{e\varepsilon}{\varepsilon_c}\right), & \varepsilon > \varepsilon_0\,, \end{cases} \tag{4}$$

where $e = 2.718$ is the base of the natural logarithm. These expressions combine the power dependence $F \propto \varepsilon^{1/2}$ at point $\varepsilon = \varepsilon_0 \approx 79$ eV (the friction force is proportional to the velocity at low energies) with the nonrelativistic Bethe formula [53] written in terms of the quantities ε_c and E_c [40, 42, 43]. For air at atmospheric pressure, we take $\varepsilon_c = 110$ eV and $E_c = 270$ kV cm^{-1}.

The field strength distributions in the GD of the experimental configurations (Figs 4a–4g) were calculated in the electrostatic approximation without taking into account the effect of the space charge of the packet [71] for a given potential difference and then renormalized taking into account the real shape of the voltage pulses (Fig. 2). The presence of a prepulse was not taken into account. Note that the static field distributions along the z-axis for the Taylor cone and the sharp needle are approximated fairly well by the dependence

$$E(z) \approx -Az^{\gamma-1} + B\,, \tag{5}$$

where A and B are some positive constants. For the Taylor cone, as follows from its definition, the exponent γ is close to 0.5. For the sharp needle, $\gamma \approx 0.21$, which, according to (2), corresponds to an opening half angle of 11° in the approximation of the real geometry of the cathode (Figs 4b and 4d) by an ideal cone. The first term on the right-hand side of (5) corresponds to the field of a conical cathode; the second constant term takes into account a decrease in the field in the near-anode region caused by the presence of a hole in the anode for delivering the RAE flow through the grid or thin foil to the sensor collector.

Let us consider the Taylor cone. To begin with, we will assume that the voltage applied to the gap is constant. It is clear from general considerations that RAEs are generated near the maximum of the 'doubled' voltage pulse (curve *3* in Fig. 2), and at the characteristic time of flight of an electron — about 60 ps — through the most important region of the strong field $z < 3$ mm (Fig. 6b), the voltage changes slightly (below, we will separately discuss the effect of the pulse shape on the runaway threshold).

Electrons at some specified potential difference U were launched with zero initial energy from the control point $z = 50$ μm. By varying U, the threshold voltage U_c was sought, at which the electrons switch to the runaway regime and reach the anode with a sufficiently high energy. Within the framework of model (3) and (4), it is convenient to consider an electron fast if its kinetic energy exceeds the value of ε_c. Then, the runaway threshold U_c corresponds to the condition $\varepsilon(D) = \varepsilon_c$ on the anode.

Table 2. Calculated RAE emission voltages (U_c) based on Laplace distributions (i.e., not taking into account the effect of space charge) of electric field. Values taking into account real shape of voltage pulses are given in parentheses.

	10 mm gap	30 mm gap
Taylor cone	$U_c = 44.5$ (45.1) kV	$U_c = 50.8$ (57.5) kV
Rounded needle	$U_c = 28.2$ kV	$U_c = 41.1$ kV
Sharp needle	$U_c = 32.5$ kV	$U_c = 48.7$ kV

As a result of calculations for air at atmospheric pressure for gaps $D = 10$ and 30 mm, we found U_c to be equal to 44.5 and 50.8 kV, respectively (Table 2). The calculated values turned out to be quite close to the experimental values of 44.6 and 55.8 kV (Table 1). If, for a short gap of 10 mm, the values of U_c almost coincided, then, for a long gap of 30 mm, the calculation gives a slightly overestimated value (by 5 kV, i.e., by 10%). This can be explained by the fact that in reality the field distributions in the GD are dynamic rather than static. For the RAE starting from the cone edge at the maximum of the voltage pulse, the field in the gap will markedly decrease at the falling trailing edge of the pulse during its movement to the anode. This effect is more pronounced for a long gap, since the RAE flight time through it is longer.

Calculations taking into account the real shape of the voltage pulses yield the threshold peak voltages of 45.1 and 57.5 kV for gaps $D = 10$ and 30 mm, respectively (Table 2, values in brackets), which correlates better with the experimental values of 44.6 and 55.8 kV (Table 1).

Thus, within the framework of a simple model (3) and (4) using Laplace field distributions, our calculations of the RAE dynamics in a GD with a Taylor cone-shaped cathode demonstrated good correlation with the experimental data. This means that our preliminary estimates from Section 2, demonstrating the insignificance of the influence of ionization processes on the conditions of RAE generation for a conical cathode with a Taylor opening angle, turned out to be correct. Experiments with such a cathode can be considered to be a 'reference' — in 'pure' conditions of the absence of a noticeable influence of the electric space charge.

Let us compare the case of needle cathodes with this 'reference.' Our analysis of needle cathodes in Section 2 indicates the importance of ionization processes and the resulting field distortion in the submillimeter cathode region due to the 'incomplete' runaway of electrons starting at the leading edge of the voltage pulse. The results of calculations with Laplace fields (Fig. 6) are given in Table 2. Evidently, the calculated threshold voltage values are noticeably lower than those for the Taylor cone — an increase in the degree of field inhomogeneity, as expected, facilitates the transition of electrons to the runaway regime. However, the opposite trend was observed in the experiments — the runaway voltages for the needles were higher than those for the Taylor cone. The differences between the experimental data and theoretical estimates are radical — approximately two times for $D = 10$ mm and one and a half times for $D = 30$ mm. At

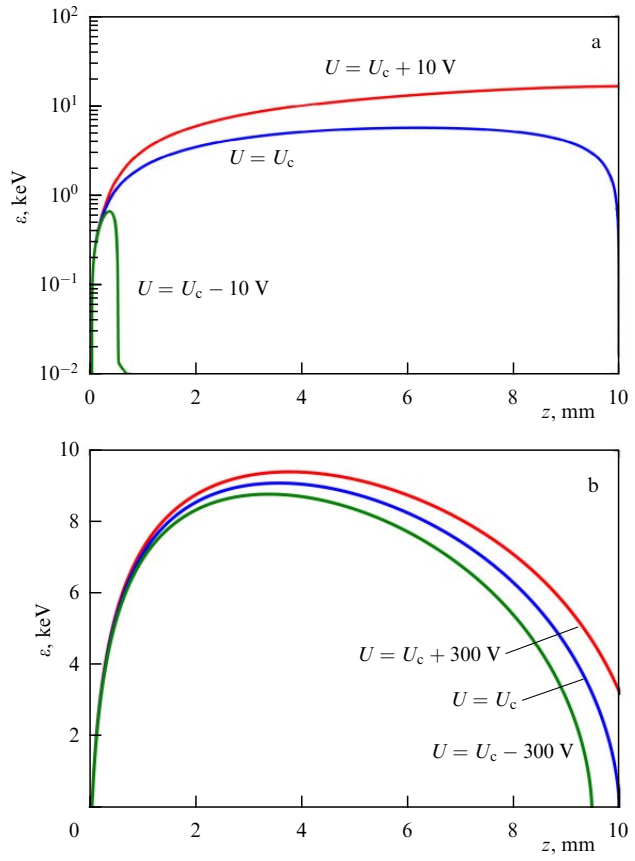

Figure 7. Dependences of kinetic energy of an electron, ε, on distance z at near-critical voltages for electron runaway ($D = 10$ mm, gas is air at atmospheric pressure). (a) Taylor cone, $U = U_c \approx 44.5$ kV (blue line) and $U = U_c \mp 10$ V (green and red lines, respectively). (b) Sharp needle, $U = U_c \approx 32.5$ kV (blue line) and $U = U_c \mp 300$ V (green and red lines, respectively).

the same time, as already discussed, for the Taylor cone there is practically no such difference.

We associate this with fundamental differences in the dynamics of free electrons at different degrees of field inhomogeneity, namely, with the fact that for the Taylor cone the runaway criterion is local, while for the needles it is nonlocal. This is illustrated by Fig. 7, which shows the dynamics of energy gain (and loss) by free electrons at several close-to-threshold voltages (U_c) for the Taylor cone and a sharp needle at the same gap length of 10 mm. Figure 7a shows the high sensitivity of the electron dynamics to the applied voltage near the runaway threshold for the Taylor cone. With a minimal change in voltage — by only ± 10 V — the behavior of the electron changes dramatically. At a subcritical voltage, the electron becomes thermal in the immediate vicinity of the cathode, at point $z \approx 0.5$ mm. In this case, the maximum energy it reaches does not exceed 0.7 kV. At a supercritical voltage, the electron reaches the anode with a high energy of more than 16.5 kV. Thus, the transition of electrons to the runaway regime has a pronounced threshold character.

Figure 7b, on the contrary, demonstrates the low sensitivity of the electron dynamics to the applied voltage for a sharp needle. With a sufficiently significant voltage deviation of ± 300 V from the critical value U_c (this deviation is thirty times greater than that considered in the previous example), the behavior of the electron does not change significantly: all three trajectories shown in Fig. 7b are close.

Table 3. Calculated values of voltages U_0 (threshold for 'incomplete' runaway, maximum energy in the gap is $2\varepsilon_c$), U_c (runaway threshold) and $U_{1/2}$ ('developed' runaway, RAE energy at anode is $0.5eU_{1/2}$) for cathodes of different configurations at $D = 10$ mm.

	U_0, kV	U_c, kV	$U_{1/2}$, kV
Taylor cone	44.23	44.50	44.64
Sharp needle	23.09	32.48	43.10

At a subcritical voltage, the electron becomes thermal near the anode, at point $z \approx 9.5$ mm; the maximum energy of the electron in the gap is 8.8 keV. At a supercritical voltage, the electron, if its motion were not limited by the anode, would become thermal at point $z \approx 10.5$ mm. In this case, the maximum energy it reaches in the gap is 9.4 keV; i.e., there are no qualitative changes, unlike the previous case with the Taylor cone.

Note that, when the voltage decreases relative to its threshold value, the electron transforms into a thermal one for the Taylor cone (Fig. 7a) near the cathode, and for the needle (Fig. 7b), it transforms near the anode. Thus, the 'bottleneck' that the electron must overcome in order to run away in the entire gap is near the cathode and the anode in the first and second cases, respectively. This indicates that for the Taylor cone the runaway criterion is local in nature (everything is determined by the electron dynamics near its starting point, near the cathode), and for the needle it is nonlocal in nature (the dynamics in the entire gap, including the near-anode region, are important).

Table 3 shows the calculated values of voltages U_0, U_c, and $U_{1/2}$ for the Taylor cone and for a sharp needle at $D = 10$ mm, characterizing the behavior of electrons during their switching to the runaway regime. Voltage U_0 corresponds to the regime when the maximum electron energy in the gap is $2\varepsilon_c$; starting from this value, a pronounced effect of 'incomplete' electron runaway occurs. Voltage U_c corresponds to our definition of the runaway threshold, $\varepsilon(D) = \varepsilon_c$. Voltage $U_{1/2}$ corresponds to the condition $\varepsilon(D) = (1/2)eU_{1/2}$, i.e., 'developed' runaway, when an electron crossing a gap as a result of collisions with gas molecules loses only half of the energy received from the electric field.

The data in Table 3 indicate a qualitative difference between the two compared cases. For the needle (the case of a highly inhomogeneous field), there is a fairly significant region of $\sim$ 10-kV width at the leading edge of the voltage pulse, in which there is 'incomplete' runaway of electrons: they begin to accelerate in a strong electric field in the immediate vicinity of the cathode, but then enter a weak field at the periphery, where they lose energy and become thermal. In this regime of motion, electrons effectively ionize the gas, initiating the formation of plasma. It can be expected that the plasma will screen the region of the enhanced field at the cathode, which will complicate the generation of RAEs and lead to an excess of the real threshold runaway voltages over those calculated for the Laplace field.

Next, as can be seen from Table 3, for the Taylor cone, a similar voltage range is negligibly small (less than 0.3 kV); i.e., the transition from the drift motion of free electrons to the runaway regime occurs abruptly. Even at $U = 44.23$ kV, electrons drift relatively slowly in the near-cathode region, reaching the maximum energy at point $z = 120$ μm, and, already at a voltage of 44.64 kV, i.e., only 0.4 kV higher, they reach the anode with an energy higher than 20 keV. In

the actual absence of the effect of 'incomplete' runaway, the influence of the electric space charge is expected to be insignificant, and the runaway threshold can be correctly calculated in the Laplace field approximation. The described results are completely consistent with our estimates from Section 2, based on the use of a model power-law field distribution in the gap [formula (1)]. The estimates fully explain the coincidence of the data in Tables 1 and 2 for the 'reference' cathode configuration in the form of a Taylor cone and their significant difference for needle cathodes.

6. Conclusions

The main objective of our study was to establish a correspondence among the experimental results, analytical estimates, and numerical calculations concerning the threshold voltages of RAE emission in GDs with cathode configurations that provide strongly differing degrees of inhomogeneity of the electric field distribution in the gap. As is typical for the analysis of threshold effects, we used measurement methods and experimental techniques that make it possible to isolate the sought-after phenomenon against the background of random processes and noise with small changes in the key parameter — the voltage pulse amplitude. The use of graphite cathodes ensured stable initiation of gas ionization processes by initial field-emission electrons. Focusing RAE flows by a magnetic field onto the collector of the current sensor made it possible to observe the appearance of electron bunches with a typical charge of fractions of a pico-coulomb. This technique for recording RAEs with an energy of tens of kiloelectron-volts is an alternative, for example, to electron-optical observations of the threshold for the occurrence of phosphor glow under their influence. Instability of subnanosecond pulses applied to the cathode after their formation by the device with spark switches allowed the fact of the occurrence of RAEs to be selected in the case of amplitude deviation at a level of one percent.

The described methods and approaches, in combination with theoretical analysis, made it possible to determine the features of electron runaway for cases of strongly and weakly inhomogeneous electric fields corresponding to the use of conical cathodes with small (up to 49.3°) and large (49.3° and higher) opening half angles. It was found that the conditions for RAE generation in the first case are nonlocal (everything is determined by the voltage applied to the gap); in the second case, they are local (for continuous acceleration of electrons in the entire gap, it is sufficient for the field strength to exceed the runaway threshold at their starting point, near the cathode). Under conditions of a highly inhomogeneous field, the effect of 'incomplete' electron runaway can play an important role: they begin to accelerate in the near-cathode region, but then, entering a weak field at the periphery, they slow down, turning into thermal ones. This process will prevent the subsequent transition of electrons to the runaway regime: it is accompanied by intense ionization of the gas and, as we believe, will lead to screening of the submillimeter region of the enhanced field with $E > E_c$ near the cathode by the forming plasma. This mechanism allows us to explain the experimental results (Section 4), according to which the runaway voltage in the case of a weakly inhomogeneous field distribution (a cathode in the form of a Taylor cone) is lower than that in the case of a strongly inhomogeneous field distribution (needle cathodes). By ignoring the effect of the space charge, an increase in the degree of field inhomogeneity would inevitably lead to a decrease in the threshold voltage of RAE emission [54].

Based on the performed studies, we can conclude that the dependence of the threshold voltage on the cone opening angle and, as a consequence, on the degree of field inhomogeneity is nonmonotonic. For a uniform field ($\alpha = 90°$ and $\gamma = 1$), the threshold voltage is obviously estimated as $U_c = E_c D$, which at $D = 10$ mm and $E_c = 270$ kV cm^{-1} yields 270 kV; i.e., it is several times greater than all the experimental values given in Table 1. When the cone is sharpened in the region of obtuse opening angles, the voltage of RAE generation decreases: for the Taylor cone ($\alpha = 49.3°$ and $\gamma = 1/2$), the experiment yields $U_c = 44.6$ kV. With further sharpening of the cone in the region of small opening angles (i.e., when it is actually transformed into a needle), the trend changes — the voltage of RAE generation increases. For needle cathodes, the experiment yields $U_c \approx 63$ kV, i.e., almost one and a half times higher than for the Taylor cone. Our analysis of the behavior of the RAEs allows us to assert that the minimum voltage will occur at a cone angle not exceeding the Taylor angle.

It should also be noted that, in [36], where the runaway conditions in an air diode with a tubular edge cathode were investigated, the experimental values of the threshold voltages were close to theoretical estimates based on an analytical consideration of the dynamics of the RAEs in a Laplace electric field [39]. As our analysis shows, this coincidence is typical of a weakly inhomogeneous (according to our classification) field. For the cathode configurations experimentally investigated in this work, it occurs only for the Taylor cone, for which the field on the symmetry axis z decreases with distance from the cone apex according to the root law $E \propto 1/\sqrt{z}$. It is noteworthy that a tubular edge cathode is characterized by a similar scaling: the field strength decreases with distance from the edge according to the same law [39, 40, 72]. The similarity of the field distributions for the Taylor cone and for the tubular edge cathode along the direction most favorable for electron runaway determines the similarity among the scenarios and conditions for the generation of RAEs.

Acknowledgments. Experimental studies of the conditions for the generation of RAEs (M I Yalandin, Sections 3 and 4) and simulation of the RAE dynamics (N M Zubarev, Section 5) were supported by the Russian Science Foundation (grant no. 23-19-00053, https://rscf.ru/project/23-19-00053/). Analysis of ionization processes in the GD with the participation of RAEs (G A Mesyats, Sections 2 and partially Section 6) was supported by the Russian Science Foundation (grant no. 19-79-30086-P, https://rscf.ru/project/23-79-33006/). The authors are grateful to their colleagues S A Shunailov, L N Lobanov, and K A Sharypov for their assistance in preparing and conducting experiments, and O V Zubareva for her assistance in numerical calculations of the RAE dynamics.

References

1. Wilson C T R *Proc. Phys. Soc. London* **37** 32D (1924)
2. Dreicer H *Phys. Rev.* **115** 238 (1959)
3. Gurevich A V *Sov. Phys. JETP* **12** 904 (1961); *Zh. Eksp. Teor. Fiz.* **39** 1296 (1960)
4. Frankel S et al. *Nucl. Instrum. Meth.* **44** 345 (1966)
5. Stankevich Yu L, Kalinin V G *Sov. Phys. Dokl.* **12** 1042 (1968); *Dokl. Akad. Nauk SSSR* **177** (1) 72 (1967)

6. Kremnev V V, Kurbatov Yu A *Sov. Phys. Tech. Phys.* **17** 626 (1972); *Zh. Tekh. Fiz.* **42** 795 (1972)
7. Tarasova L V et al. *Sov. Phys. Tech. Phys.* **19** 351 (1974); *Zh. Tekh. Fiz.* **44** 564 (1974)
8. Mesyats G A, Bychkov Yu I, Kremnev V V *Sov. Phys. Usp.* **15** 282 (1972); *Usp. Fiz. Nauk* **107** 201 (1972)
9. Mesyats G A et al. *Tech. Phys. Lett.* **34** 169 (2008); *Pis'ma Zh. Tekh. Fiz.* **34** (4) 71 (2008)
10. Tarasenko V F et al. *Rev. Sci. Instrum.* **83** 086106 (2012)
11. Tarasenko V F, Rybka D V *High Voltage* **1** (1) 43 (2016)
12. Mesyats G A et al. *Appl. Phys. Lett.* **116** 063501 (2020)
13. Tarasenko V F, Beloplotov D V, Sorokin D A *Tech. Phys.* **67** 586 (2022); *Zh. Tekh. Fiz.* **92** 694 (2022)
14. Mesyats G A et al. *IEEE Electron Device Lett.* **43** 627 (2022)
15. Mesyats G A et al. *IEEE Trans. Plasma Sci.* **36** 2497 (2008)
16. Tarasenko V F et al. *Tech. Phys. Lett.* **29** 879 (2003); *Pis'ma Zh. Tekh. Fiz.* **29** (21) 1 (2003)
17. Akishev Yu et al. *J. Phys. D* **51** 394003 (2018)
18. Tarasenko V F et al. *JETP Lett.* **102** 350 (2015); *Zh. Eksp. Teor. Fiz.* **102** 388 (2015)
19. Kozyrev A et al. *Europhys. Lett.* **114** 45001 (2016)
20. Lobanov L N et al. *IEEE Electron Device Lett.* **44** 1748 (2023)
21. Alekseev S B, Orlovskii V M, Tarasenko V F *Tech. Phys. Lett.* **29** 411 (2003); *Pis'ma Zh. Tekh. Fiz.* **29** (10) 29 (2003)
22. Tarasenko V F, Orlovskii V M, Shunailov S A *Russ. Phys. J.* **46** 325 (2003); *Izv. Vyssh. Uchebn. Zaved. Fiz.* **46** (3) 94 (2003)
23. Babich L P, Loiko T V, Tsukerman V A *Sov. Phys. Usp.* **33** 521 (1990); *Usp. Fiz. Nauk* **160** (7) 49 (1990)
24. Korolev Yu D, Mesyats G A *Fizika Impul'snogo Proboya Gazov* (Physics of Pulsed Gas Breakdown) (Moscow: Nauka, 1991)
25. Dwyer J R, Smith D M, Cummer S A *Space Sci. Rev.* **173** 133 (2012)
26. Babich L P *High-Energy Phenomena in Electric Discharges in Dense Gases*: *Theory, Experiment, and Natural Phenomena* (Arlington, TX: Futurepast, 2003)
27. Mesyats G A *Phys. Usp.* **49** 1045 (2006); *Usp. Fiz. Nauk* **176** 1069 (2006)
28. Lisenkov V V et al. *Tech. Phys.* **63** 1872 (2018); *Zh. Tekh. Fiz.* **88** 1912 (2018)
29. Bakhov K I, Babich L P, Kutsyk I M *IEEE Trans. Plasma Sci.* **28** 1254 (2000)
30. Babich L, Bochkov E *J. Phys. D* **54** 465205 (2021)
31. Wen Z et al. *IEEE Trans. Plasma Sci.* **51** 2124 (2023)
32. Peterson L R, Green A E S *J. Phys. B* **1** 1131 (1968)
33. Mesyats G A et al. *Plasma Phys. Rep.* **38** 29 (2012); *Fiz. Plazmy* **38** 34 (2012)
34. Shao T et al. *Laser Part. Beams* **30** 369 (2012)
35. Erofeev M V et al. *Tech. Phys.* **58** 200 (2013); *Zh. Tekh. Fiz.* **83** (2) 52 (2013)
36. Zubarev N M et al. *J. Phys. D* **51** 284003 (2018)
37. Beloplotov D V et al. *Tech. Phys.* **66** 548 (2021); *Zh. Tekh. Fiz.* **91** 589 (2021)
38. Lobanov L N et al. *Phys. Plasmas* **31** 063102 (2024)
39. Zubarev N M, Mesyats G A, Yalandin M I *JETP Lett.* **105** 537 (2017); *Pis'ma Zh. Eksp. Teor. Fiz.* **105** 515 (2017)
40. Zubarev N M, Zubareva O V, Yalandin M I *Electronics* **11** 2771 (2022)
41. Mamontov Yu I, Zubarev N M, Uimanov I V *IEEE Trans. Plasma Sci.* **49** 2589 (2021)
42. Zubarev N M, Zubareva O V, Yalandin M I *Tech. Phys.* **68** 1204 (2023); *Zh. Tekh. Fiz.* **93** 1298 (2023)
43. Zubarev N M, Zubareva O V, Yalandin M I *Tech. Phys. Lett.* **49** (9) 64 (2023); *Pis'ma Zh. Tekh. Fiz.* **49** (18) 24 (2023)
44. Tkachev A N, Yakovlenko S I *Tech. Phys. Lett.* **29** 683 (2003); *Pis'ma Zh. Tekh. Fiz.* **29** (16) 54 (2003)
45. Tkachev A N, Yakovlenko S I *JETP Lett.* **77** 221 (2003); *Pis'ma Zh. Eksp. Teor. Fiz.* **77** 264 (2003)
46. Tarasenko V F, Yakovlenko S I *Phys. Usp.* **47** 887 (2004); *Usp. Fiz. Nauk* **174** 953 (2004)
47. Zhang C et al. *Laser Part. Beams* **31** 353 (2013)
48. Baksht E Kh, Burachenko A G, Tarasenko V F *Tech. Phys.* **60** 1645 (2015); *Zh. Tekh. Fiz.* **85** (11) 73 (2015)
49. Gashkov M A et al. *JETP Lett.* **113** 370 (2021); *Pis'ma Zh. Eksp. Teor. Fiz.* **113** 370 (2021)
50. Mesyats G A et al. *Electronics* **11** 248 (2022)
51. Yalandin M I et al. *IEEE Trans. Instrum. Measur.* **72** 1008808 (2023) https://doi.org/10.1109/TIM.2023.3307183
52. Askar'yan G A *Trudy Fiz. Inst. Akad. Nauk SSSR* **66** 66 (1973)
53. Bethe H *Ann. Physik* **397** 325 (1930)
54. Zubarev N M, Zubareva O V, Yalandin M I *Dokl. Phys.* **68** 279 (2023); *Dokl. Ross. Akad. Nauk. Fiz. Tekh. Nauki* **512** (1) 5 (2023)
55. Taylor G I *Proc. R. Soc. London A* **280** 383 (1964)
56. Zhakin A I *Phys. Usp.* **56** 141 (2013); *Usp. Fiz. Nauk* **183** 153 (2013)
57. Zubarev N M *JETP Lett.* **73** 544 (2001); *Pis'ma Zh. Eksp. Teor. Fiz.* **73** 613 (2001)
58. Suvorov V G, Zubarev N M *J. Phys. D* **37** 289 (2004)
59. Schonland B F J *Proc. R. Soc. London A* **104** 235 (1923)
60. Kunhardt E E, Byszewski W W *Phys. Rev. A* **21** 2069 (1980)
61. Belomyttsev S Ya et al. *Tech. Phys. Lett.* **34** 367 (2008); *Pis'ma Zh. Tekh. Fiz.* **34** (9) 10 (2008)
62. Levko D et al. *J. Appl. Phys.* **111** 013303 (2012)
63. Zubarev N M et al. *Plasma Sources Sci. Technol.* **29** 125008 (2020)
64. Shpak V G et al. *Instrum. Exper. Techn.* **36** (1) 106 (1993); *Prib. Tekh. Eksp.* (1) 149 (1993)
65. Yalandin M I et al. *IEEE Trans. Plasma Sci.* **30** 1700 (2002)
66. Sharypov K A et al. *Rev. Sci. Instrum.* **85** 125104 (2014)
67. Belomyttsev S Ya et al. *J. Appl. Phys.* **119** 023304 (2016)
68. Korovin S D et al. *Tech. Phys. Lett.* **30** 813 (2004); *Pis'ma Zh. Tekh. Fiz.* **30** (19) 30 (2004)
69. Yalandin M I et al. *IEEE Trans. Plasma Sci.* **38** 2559 (2010)
70. Wu Y C et al. *Rev. Sci. Instrum.* **83** 026101 (2012)
71. Fomel B M, Tiunov M A, Yakovlev V P "SAM — an interactive code for electron gun evaluation," Budker INP 96-11 (Novosibirsk: Budker Institute of Nuclear Physics SB RAS, 1996)
72. Belomyttsev S Ya, Romanchenko I V, Rostov V V *Russ. Phys. J.* **51** 299 (2008); *Izv. Vyssh. Uchebn. Zaved. Fiz.* (3) 71 (2008)